Journal of Integrative Agriculture 2026, 25(7): 2847–2858

Available online at ScienceDirect

Journal of Integrative Agriculture



RESEARCH ARTICLE

Functional analysis of *CsAGL6* in flower development and pigmentation in cucumber (*Cucumis sativus* L.)

Li Qin[1, 3*], Zheyuan Liu[1, 3*], Shuai Li[1, 2, 4], Guanghua Cai[1, 2], Jie Wang[1], Xueyong Yang[1], Jinjing Sun[1#]

[1] *State Key Laboratory of Vegetable Biobreeding, Institute of Vegetables and Flowers, Chinese Academy of Agricultural Sciences, Beijing 100081, China*
[2] *Genome Analysis Laboratory of the Ministry of Agriculture and Rural Affairs, Agricultural Genomics Institute at Shenzhen, Chinese Academy of Agricultural Sciences, Shenzhen 518124, China*
[3] *National Nanfan Research Institute (Sanya), Chinese Academy of Agricultural Sciences, Sanya 572024, China*
[4] *Shandong Key Laboratory of Bulk Open-field Vegetable Breeding, Key Laboratory of Huang Huai Protected Horticulture Engineering of Ministry of Agriculture and Rural Affairs, Institute of Vegetables, Shandong Academy of Agricultural Sciences, Jinan 250100, China*

Highlights

- *CsAGL6* participates in sepal and petal development by regulating *CAL* and *SEP4* in cucumber.
- *CsAGL6* affects petal pigmentation by modulating genes involved in chlorophyll biosynthesis and chloroplast development in cucumber.

Abstract

Cucumber (*Cucumis sativus* L.) is a major vegetable crop worldwide, and its yield and quality are closely linked to flower development. AGAMOUS-LIKE 6 (AGL6), a member of the ancient MADS-box transcription factor family, plays a crucial role in flower development. However, the specific functions of its homolog in cucumber remain poorly understood. In this study, we demonstrate that *CsAGL6* is predominantly expressed in flowers, with high expression levels observed in all floral organ primordia during the early stages of floral development. The petals of *Csagl6* mutants exhibit a greener color compared to wild-type plants, along with a significant increase in total chlorophyll content. Additionally, the mutants show abnormal petal morphology, including changes in size and shape, as well as enlarged sepals resembling leaves occasionally. Molecular analysis reveals that *CAULIFLOWER* (*CAL*) and the E-class gene *SEPALLATA 4* (*SEP4*) are significantly downregulated in the mutants, while the chlorophyll synthesis gene *Early Light-Induced Protein 1* (*ELIP1*) and several stress-related genes in the chloroplasts are dramatically upregulated. Our findings provide novel insights into the functional role of *CsAGL6* in regulating sepal and petal development, and offer a potential avenue for understanding the genetic control of flower pigmentation and organ morphology in *Cucumis* species.

Keywords: cucumber, flower development, *CsAGL6*

1. Introduction

Flowering represents a critical transition from vegetative to reproductive growth and plays an essential role in the propagation of offspring in angiosperms. The genetic regulation of flower development has been extensively studied, with a significant contribution coming from various floral organ mutants in different species (Elliot *et al.* 1989; Mizukami and Ma 1992; Angenent and Colombo 1996; Pelaz *et al.* 2001; Favaro *et al.* 2003; Pinyopich *et al.* 2003; Ditta *et al.* 2004). In 1991, Coen and Meyerowitz (1991) proposed the classical ABC model of flower development, which laid the foundation for understanding the genetic control of floral organ identity. As research progressed, this model was further expanded into the ABCDE model (Angenent and Colombo 1996; Pelaz *et al.* 2000; Theißen 2001; Favaro *et al.* 2003; Pinyopich *et al.* 2003; Ditta *et al.* 2004). In this extended framework, the E-class genes are involved in regulating the development of floral organs in all four whorls,

Received 28 March 2025; Received in revised form 9 July 2025; Accepted 23 September 2025; Available online 13 November 2025
Li Qin, E-mail: qinliqinfen@163.com; Zheyuan Liu, E-mail: hnlzy1028@163.com; #Correspondence Jinjing Sun, E-mail: sunjinjing@caas.cn
* These authors contributed equally to this study.

© 2026 CAAS. Publishing services by Elsevier B.V. on behalf of KeAi Communications Co. Ltd. This is an open access article under the CC BY-NC-ND license (http://creativecommons.org/licenses/by-nc-nd/4.0/). Peer review under responsibility of Editorial Board of *Journal of Integrative Agriculture*.
doi: 10.1016/j.jia.2025.11.012

working in concert with other classes of genes (Theißen 2001; Ditta *et al.* 2004; Theißen *et al.* 2016). Specifically, A-class genes, together with E-class genes, regulate sepal development; A, B and E-class genes collaborate to control petal development; B, C and E-class genes are responsible for stamen development; C and E-class genes govern carpel development; and C, D and E-class genes are involved in ovule development (Causier *et al.* 2010; Irish 2010; Bowman *et al.* 2012; Theißen *et al.* 2016). Notably, with the exception of the A-class gene *APETALA2* (*AP2*) and its homologs, all the floral organ identity genes in the ABCDE model belong to the MADS-box gene family (Irish 2010).

AGAMOUS-LIKE 6 (*AGL6*) is an ancient subfamily within the MADS-box gene family. Phylogenetic analyses suggest that *AGL6* belongs to the *SEPALLATA* (*SEP*)/*AGL6*/*APETALA1* (*AP1*)/*FLOWERING LOCUS C* (*FLC*) superclade, with *AGL6* being more closely related to *SEP*, forming a sister clade (Purugganan 1997; Becker and Theißen 2003; Hileman *et al.* 2006). While *AGL6*, *SEP*, *AP1*, and *FLC* are present in angiosperms, *AGL6* is the only member of this group found in gymnosperms (Dreni and Zhang 2016). The *AGL6* lineage has undergone multiple duplications throughout plant evolution (Viaene *et al.* 2010). These duplication events often lead to structural variations in the genes, resulting in sub-functionalization or the emergence of new functions, thereby contributing to the functional diversity observed in *AGL6* (Dreni and Zhang 2016; Yu *et al.* 2016).

In dicotyledons, the model plant *Arabidopsis thaliana* contains two members of the *AGL6* subfamily, *AGL6* and *AGL13*. Previous studies have shown that loss of *AGL6* function in *Arabidopsis* does not cause apparent developmental abnormalities; however, overexpression of *AGL6* leads to early flowering phenotypes under both long and short-day conditions (Koo *et al.* 2010). Additionally, these overexpressing plants produce terminal flowers at the apex of the inflorescence, with altered numbers and morphologies of floral organs (Koo *et al.* 2010). A genetic screen for leaf movement mutants further revealed that *AGL6* plays a role in circadian clock regulation by modulating the expression of *ZEITLUPE* (*ZTL*) (Yoo *et al.* 2011). Analysis of natural allelic variation and epistatic interactions has shown that *AGL6* also influences stem branch number by promoting axillary bud formation (Huang *et al.* 2012). In contrast, *AGL13* primarily regulates the morphogenesis of male and female gametes, promoting the development of pollen and ovules (Hsu *et al.* 2014).

Studies in tomato (*Solanum lycopersicum* L.) have shown that under high-temperature stress, the wild-type plants fail to fertilize due to abnormal male gametophyte development, whereas the *SlAGL6*-silenced mutants produce a large number of high-quality seedless fruits (Klap *et al.* 2017). These findings highlight its potential for parthenocarpic breeding. Further investigations have indicated that silencing *SlAGL6* results in abnormalities in sepal fusion and an elongation of petals, likely due to its impact on the expression of genes involved in boundary formation, sepal and petal development (Yu *et al.* 2017).

In the monocotyledon group, the gramineous model plant rice (*Oryza sativa* L.) contains two *AGL6* genes, *OsMADS6* and *OsMADS17*. All floral organs except lemma homeotically transform into lemma-like organs, the determinacy of the floral meristem is lost and mosaic organs are observed in *Osmads6* mutants (Ohmori *et al.* 2009; Duan *et al.* 2012). Overexpression of *OsMADS6* results in an excess of lodicule-, stamen- and carpel-like organs (Duan *et al.* 2012). The loss-of-function mutant of *OsMADS17* does not show significant morphological abnormalities; however, the *Osmads6 Osmads17* double mutant displays a more severe phenotype than the *Osmads6* single mutant, suggesting functional redundancy between the two genes, with *OsMADS6* playing a more dominant role (Ohmori *et al.* 2009). Additionally, a newly identified *Osmads6* mutant presents abnormal glume morphology, with grains that are wider and shorter, an increase in protein and soluble sugar levels, a reduction in amylose content, and an elevated gelatinization temperature, indicating that *OsMADS6* is crucial for influencing both rice grain yield and quality (Yu *et al.* 2020).

In wheat (*Triticum aestivum* L.), the genome has three *AGL6* homoeologous genes, *TaAGL6-A*, *TaAGL6-B* and *TaAGL6-D*, and they are strongly expressed in floral tissues with similar expression patterns (Su *et al.* 2019). RNAi-mediated silencing of these genes does not induce significant phenotypic changes during the vegetative phase, however, during the reproductive stage, the expression of *TaAP3* (*APETALA3*) is markedly downregulated, resulting in abnormalities in the number and morphology of stamens (Su *et al.* 2019). Recent studies have demonstrated that *TaAGL6* plays a critical role in the development of all four floral whorls, in addition, loss of *TaAGL6* function leads to reduced fertility in floret, with a dose-dependent effect on fertility and spikelet number (Kong *et al.* 2022).

In the ornamental orchids, B-class and AGL6 proteins have been shown to form complexes that modify the structure of the lower outer sepals and assist in positioning the lip at the flower's center (Hsu *et al.* 2021). Furthermore, these complexes regulate anthocyanin accumulation and pigmentation, influencing flower color and promoting red spot formation in the perianth (Li *et al.* 2020; Hsu *et al.* 2021).

Cucumber (*Cucumis sativus* L.), a member of the Cucurbitaceae family, is an annual herbaceous vegetable crop that is widely cultivated worldwide. The fruit of cucumber develops from the ovary of the female flower, making normal flower development crucial for ensuring both yield and quality. Previous studies have demonstrated that *AGL6* and its homologs play a critical role in regulating flower development, and multitudinous functional differentiation occurs among various species. However, to date, research on the cloning and expression analysis of *AGL6* homolog has been limited to bitter gourd (*Momordica charantia* L.) among cucurbit species (Peng *et al.* 2008). In that study, *McAG6* (an *AGL6*-like gene) was cloned from female buds of bitter gourd based on conserved MADS-box sequences. Transcripts of *McAG6* were primarily detected in male buds, female buds and shoot apices. In addition, *McAG6* exhibited very low expression in young fruit, carpel, and stamen, moderate in calyx and petal, and high in shoot apex. This expression pattern suggests that *McAG6* may play a role in regulating bitter gourd floral development (Peng *et al.* 2008). So regrettably, no *AGL6* ortholog function has been reported in Cucurbitaceae. Therefore, investigating the function of the *AGL6* homolog in cucumber will help its

clarify functional differentiation within the Cucurbitaceae family and provide deeper insights into the molecular mechanisms underlying cucumber flower development. Such findings are not only essential for understanding the biological processes of cucumber but also offer valuable theoretical references for agricultural production and breeding.

In this study, the expression pattern of *CsAGL6* was analyzed using real-time quantitative PCR (RT-qPCR) and in situ hybridization. Two homozygous mutants with loss-of-function of *CsAGL6* were generated using CRISPR/Cas9 system and *Agrobacterium*-mediated genetic transformation. These mutants exhibited delayed yellowing of petal color, abnormal petal shape and size, and enlarged sepals with a noticeable leaf-like morphology. Transcriptome sequencing analysis suggested that *CsAGL6* plays a crucial role in cucumber floral organ development by regulating the expression of A-class and E-class related genes. Additionally, *CsAGL6* appears to influence petal color by modulating chlorophyll synthesis. This research provides new insights into the functional roles of *CsAGL6* in regulating sepal and petal development and offers a potential avenue for understanding the genetic control of flower pigmentation and organ morphology in *Cucumis* species.

2. Materials and methods

2.1. Plant materials and growth conditions

The cucumber materials used in this study are the South China type monoecious inbred line CU2 obtained from Hunan Xingshu Seed Industry Co., Ltd. (Changsha, Hunan, China). These seeds were planted in a greenhouse at the Vegetable and Flower Research Institute of the Chinese Academy of Agricultural Sciences in Beijing. Standardized water and fertilizer management were uniformly applied by the farm throughout the study.

The tobacco used for the subcellular localization experiment is *N. benthamiana*, which is preserved in our laboratory and grown under controlled conditions in a climate chamber with a 16-h light/8-h dark cycle.

2.2. Multiple sequence alignment and phylogenetic analysis

Homologs of the *Arabidopsis* AGL6 protein in cucurbit species were identified using a BLAST search with the full-length amino acid sequence of AGL6 in the Cucurbit Genomics Database (http://www.cucurbitgenomics.org/). Additionally, homologous proteins from other species were retrieved through BLAST searches in the NCBI (National Center for Biotechnology Information) database. A multiple sequence alignment of the identified proteins was performed using ClustalX software. The phylogenetic analysis was generated using MEGA11 with the Neighbor-Joining (NJ) method, and bootstrap values were calculated from 1,000 replicates for statistical robustness. The species and gene information used for multiple sequence alignment and phylogenetic tree construction are provided in Appendix A.

2.3. RNA extraction, cDNA synthesis, and real-time quantitative PCR (RT-qPCR)

Samples were collected from 10 distinct tissues of cucumber plants at the 20th node stage. The tissues included leaves, young stems, and shoot apices (with visible leaves, tendrils and flower buds removed), as well as male buds, male flowers (on the day of anthesis), female buds, ovary-free female flowers (on the day of anthesis), ovaries (on the day of anthesis), male flower pedicels and female flower pedicels (on the day of anthesis). Four plants were pooled to constitute one biological replicate. Total RNA was extracted using the TRIzol (15596018, Ambion, Austin, USA) reagent and treated with DNase I to eliminate genomic DNA contamination. First-strand cDNA synthesis was performed using the GoScript™ reverse transcriptase (A2791, Promega, Madison, USA). RT-qPCR was conducted using the TB Green® Premix Ex Taq™ II FAST qPCR Kit (CN830A, TaKaRa, Tokyo, Japan). The expression of *CsACTIN2* (*CsaV3_6G041900*) served as the internal reference, and relative gene expression levels were calculated using the $2^{-\Delta Ct}$ method (Schmittgen and Livak 2008). The experiment comprised four biological replicates, with each biological replicate analyzed in triplicate (technical replicates). Primers were designed using the NCBI Primer-BLAST tool, and their sequences are provided in Appendix B.

2.4. *In situ* hybridization

The *in situ* hybridization was carried out following previously described protocols (Wang *et al*. 2023). Briefly, using a 500 bp fragment of the *CsAGL6* CDS region as a template, sense and antisense RNA probes were synthesized *via in vitro* transcription, with the sense probe serving as a negative control. The shoot apices, male flower buds (less than 3 mm in size), and female flower buds (less than 1 cm in size) were collected from cucumber plants grown to the 20th node. These tissues were fixed in 4% paraformaldehyde (PFA) solution and subjected to vacuum infiltration until all tissues settled at the bottom of the tube.

The fixed tissues were then dehydrated through a graded ethanol series (30%, 50%, 70%, 85%, 95%, and twice in 100%), with each step performed in an ice bath with gentle shaking for 1–2 h. Subsequently, the tissues were embedded in Steedman's wax, ensuring complete infiltration, and polymerized at room temperature for 36 h. The resulting wax blocks were stored at –20°C. Individual tissue blocks were sectioned into ribbons with a thickness of 20 μm, placed in RNase-free petri dishes, and dissolved in anhydrous ethanol.

Tissue sections were isolated using RNase-free disposable syringe needles and transferred to a 100 μm cell filter submerged in anhydrous ethanol. These sections were either processed immediately for hybridization or stored overnight at 4°C. Following hybridization, washing, and color development, images were captured using a Leica microscope (DM5500 B). Primer information is provided in Appendix B.

2.5. Subcellular localization of CsAGL6

The coding sequence of *CsAGL6*, excluding the termination codon, was cloned into the Super1300 plasmid fused to the green fluorescent protein (GFP) coding sequence, using *Spe*I and *Kpn*I restriction sites. The resulting recombinant plasmid was confirmed by sequencing and introduced into

Agrobacterium tumefaciens strain GV3101 for tobacco epidermal cells injection. Images were captured using a Leica confocal laser scanning microscope (TCS SP8), with excitation at a wavelength of 488 nm. The primer sequences are listed in Appendix B.

2.6. CRISPR/Cas9 vector construction

A 19 bp single-guide RNA (sgRNA) target for *CsAGL6* was designed using the CRISPR-GE online tool (http://skl.scau.edu.cn/), and its specificity was verified *via* BLAST analysis against the cucumber genome database. PCR amplification was performed using the pCBC-DT1T2 plasmid (Xing *et al.* 2014) as a template, and the target fragment of *CsAGL6* was generated by incorporating the homology arms of the pCBC-DT1T2 plasmid at both ends of the target sequence. The purified PCR product was subsequently inserted into the linearized pBSE402 vector using the *Bsa*I restriction enzyme. The resulting recombinant plasmid, pBSE402-AGL6, was confirmed by sequencing and introduced into *A. tumefaciens* strain EHA105 for cucumber genetic transformation. Primer information is provided in Appendix B.

2.7. Cucumber genetic transformation

The genetic transformation of cucumber was performed as previously description (Xin *et al.* 2022). Briefly, cucumber seeds of the CU2 variety were sterilized and sown onto germination medium, followed by incubation in the dark at 28°C for 24 h. A portion (approximately one-third) of the distal end of each cotyledon was excised, and the hypocotyl was removed, creating a U-shaped wound at the proximal end of the cotyledons. An additional incision was made at the U-shaped wound using a scalpel to separate the cotyledons and obtain suitable explants. *Agrobacterium* that had been pre-activated and proliferated was resuspended in inoculation solution and adjusted to an optical density (OD) of 0.2 at 600 nm for infection.

The cotyledon explants were subjected to ultrasound treatment at 100 W for 30 s to facilitate wound formation and enhance infection efficiency. The explants were then placed into a 20 mL syringe, and an appropriate volume of *Agrobacterium* suspension was drawn in, with air bubbles and excess liquid expelled. The syringe piston was pushed to the 10 mL mark, and the needle was sealed with a rubber stopper. A vacuum was created by pulling the piston back to the 20 mL mark and holding it for 90 s, followed by gentle shaking to ensure even distribution of pressure on the explants. The vacuum treatment was repeated to further improve infection efficiency.

The explants infected with *Agrobacterium* were transferred evenly onto co-cultivation medium, which was covered with a layer of filter paper. The explants were then incubated in the dark at 23°C for 3 d. After co-cultivation, the explants were transferred to shoot induction medium and cultured under light conditions for 3–4 weeks to promote shoot differentiation. The GFP-positive buds, identified using a fluorescence microscope, were selected for further regeneration and transferred to root induction medium. Transgenic positive seedlings with well-developed roots were carefully removed from the medium, and any adhering medium on the roots was thoroughly washed off. The seedlings were then transferred to sterilized soil for acclimatization and hardening in a light incubator. Once the seedlings developed robust root systems, they were transferred to a controlled climate room for further cultivation until they were ready for pollination and seed setting.

2.8. Extraction and quantitation of chlorophyll

To extract and quantify chlorophyll, weigh 0.5 g of fresh petals from wild-type and mutant plants 1 d before flowering. Place the petals in a mortar and add a small amount of calcium carbonate powder and quartz sand, followed by 5 mL of 95% ethanol. Grind the mixture thoroughly, then add an additional 10 mL of 95% ethanol and continue grinding. Incubate the homogenate in the dark for 5 min. Transfer the mixture to a 50-mL centrifuge tube and centrifuge at 5,000 r min^{-1} for 5 min. Measure the absorbance of the supernatant at 665 and 649 nm using a spectrophotometer. Total chlorophyll was calculated using the following formulas: Chlorophyll concentration (mg L^{-1})=18.08×A_{649}+6.63×A_{665}; Total chlorophyll (mg g^{-1})=(Chlorophyll concentration×Extraction volume)/Sample weight.

2.9. Transcriptome analysis

Shoot apices (removing visible leaves, tendrils, and flower buds) of wild-type and mutant plants, grown to the 20th node, were collected for transcriptome sequencing. Four biological replicates were prepared for each group, with at least four plants pooled per replicate. Total RNA was extracted using the TRIzol (15596018, Ambion, Austin, USA) reagent, and high-throughput paired-end sequencing (PE150) was performed on the Illumina NovaSeq 6000 platform. RNA-seq libraries were constructed, and the sequencing yielded approximately 10 Gb of data. The raw reads were processed to remove adapters and low-quality sequences, ensuring high-quality data for subsequent analysis.

Gene expression levels were quantified as fragments per kilobase of transcript per million mapped fragments (FPKM). Pearson correlation coefficients (PCC) between samples were calculated using R packages, and correlation plots were generated. Statistical analyses were performed using Python scripts. Differential gene expression analysis was carried out using the R package DESeq2, with a significance threshold set at P<0.05 and a fold change of ≥2.0 for upregulated/downregulated genes.

3. Results

3.1. Sequence analysis of CsAGL6

To investigate the function of *AGL6* homolog in cucumber, BLAST searches were conducted in the Cucurbitaceae genome database using the full-length amino acid sequence of AGL6 from *Arabidopsis*. The results identified *CsaV3_6G006010* as the gene with the highest similarity to *Arabidopsis AGL6* (E=9.27e−108). In addition, *CsaV3_6G006010* showed the best match to *AGL6* in the Arabidopsis Information Resource (TAIR) database, followed by *AGL13*. Since *AGL6* and *AGL13* are members of the *AGL6* subfamily in *Arabidopsis*, *CsaV3_6G006010* was

designated as *CsAGL6*. The full-length coding sequence of *CsAGL6* was subsequently cloned from the monoecious cucumber inbred line CU2. Gene structure analysis revealed that *CsAGL6* spans 4,817 bp, contains eight exons, and includes a 744 bp open reading frame encoding a protein of 247 amino acids.

A multiple sequence alignment was performed on AGL6 protein sequences from 14 species, including cucumber (*Cucumis sativus*), melon (*Cucumis melo*), watermelon (*Citrullus lanatus*), winter squash (*Cucurbita moschata*), wax gourd (*Benincasa hispida*), bitter gourd (*Momordica charantia*), *Arabidopsis* (*Arabidopsis thaliana*), cotton (*Gossypium hirsutum*), papaya (*Carica papaya*), rosary pea (*Abrus precatorius*), grape (*Vitis vinifera*), tomato (*Solanum lycopersicum*), rice (*Oryza sativa*), and corn (*Zea mays*) (Fig. 1). And a phylogenetic tree was constructed also based on the AGL6 protein sequences from these 14 species (Appendix C). The multiple sequence alignment results revealed that the CsAGL6 protein contains two conserved domains characteristic of MADS-box transcription factors, the DNA-binding MADS-box region and the K-box, which is involved in protein-protein interactions, confirming its classification as a typical MADS-box protein (Fig. 1). Additionally, the C-terminal region of CsAGL6 contains AGL6 motifs I and II (Fig. 1). Phylogenetic analysis further confirmed that CsAGL6 clusters within the conserved AGL6 clade (Appendix C).

3.2. Expression pattern of *CsAGL6*

To investigate the expression pattern of *CsAGL6*, RT-qPCR was performed on RNA extracted from various

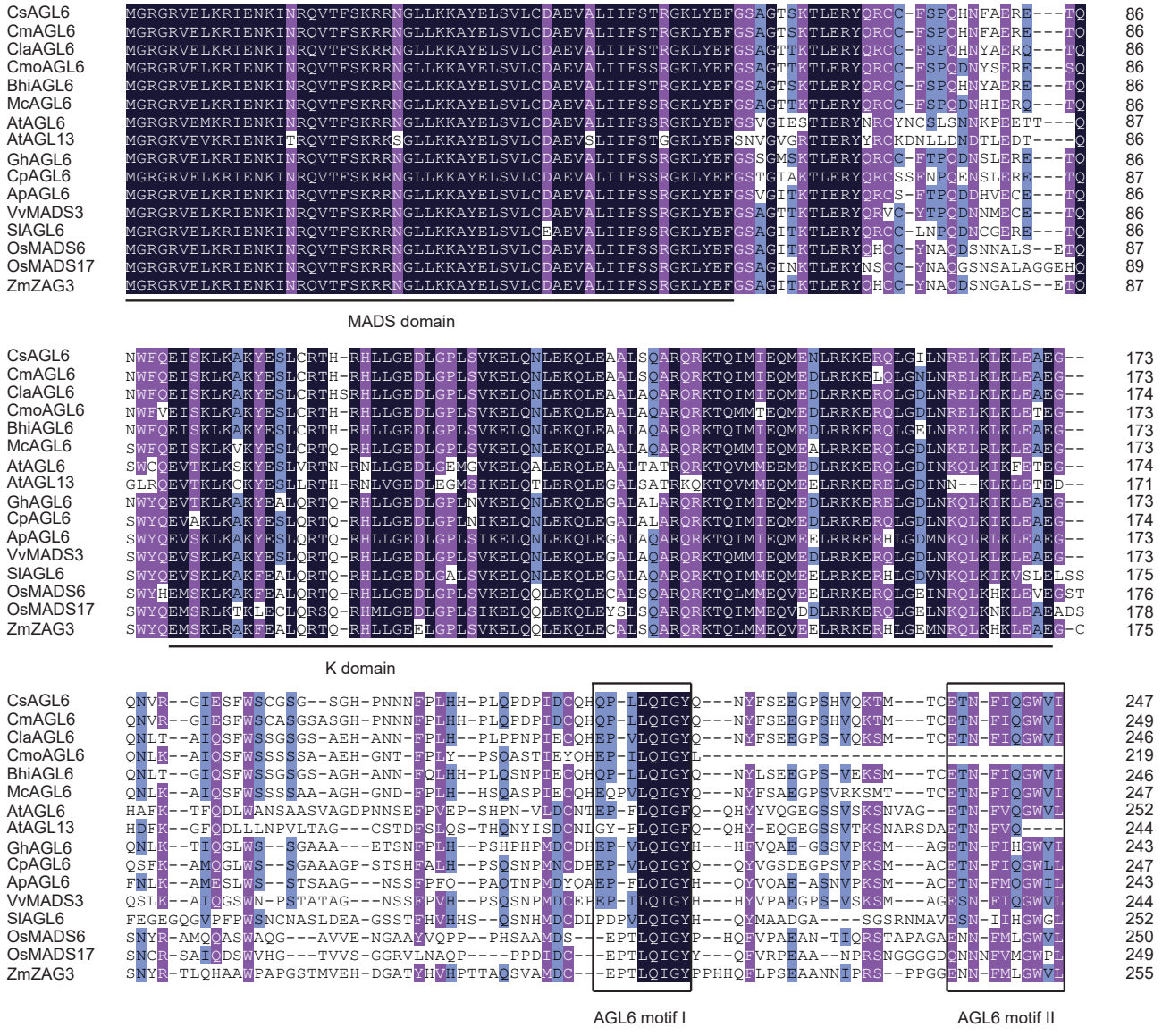


Fig. 1 Sequence alignment of CsAGL6 and AGL6 proteins from other representative species. The MADS domain and K domain regions are underlined, while AGL6 motifs I and II are boxed. Species abbreviations are as follows: Cs (*Cucumis sativus*), Cm (*Cucumis melo*), Cla (*Citrullus lanatus*), Cmo (*Cucurbita moschata*), Bhi (*Benincasa hispida*), Mc (*Momordica charantia*), At (*Arabidopsis thaliana*), Gh (*Gossypium hirsutum*), Cp (*Carica papaya*), Ap (*Abrus precatorius*), Vv (*Vitis vinifera*), Sl (*Solanum lycopersicum*), Os (*Oryza sativa*), Zm (*Zea mays*).

tissues, including leaves, young stems, shoot apices, male buds (mb), male flowers at anthesis (mf), female buds (fb), female flowers at anthesis without ovary (ff), ovary at anthesis (ov), male flower stalks at anthesis (mfs), and female flower stalks at anthesis (ffs) in cucumber. The results revealed that *CsAGL6* is predominantly expressed in the shoot apex (with some early flower buds invisible to the naked eyes), male buds, male flowers, female buds, and female flowers, with the highest expression levels observed in male and female flowers. In contrast, low levels of *CsAGL6* transcripts were detected in the ovary, while no significant expression was found in leaves, young stems, male flower pedicels, or female flower pedicels (Fig. 2-A). These findings suggest that *CsAGL6* may play a key role in flower development in cucumber. Furthermore, subcellular localization analysis showed that CsAGL6 is localized to the nucleus (Fig. 2-B), consistent with its classification as a transcription factor.

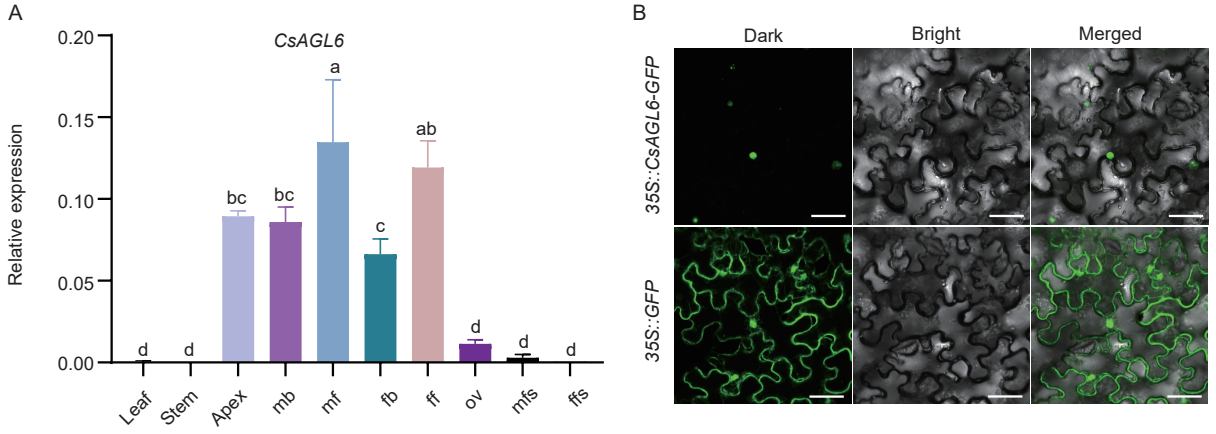


Fig. 2 Expression analysis and subcellular localization of *CsAGL6*. A, RT-qPCR analysis of *CsAGL6* expression across different tissues. Tissues include leaf, stem, apex, male buds (mb), male flowers at anthesis (mf), female buds (fb), female flowers at anthesis without ovary (ff), ovary at anthesis (ov), male flower stalks at anthesis (mfs), and female flower stalks at anthesis (ffs). Data are presented as mean±SEM (n=4). Significant differences determined by Duncan's test (P<0.05), are represented by different lowercase letters above the error bars. B, subcellular localization of CsAGL6 in tobacco cells. *35S::GFP* construct was used as a control. Fluorescence signals were observed 48 h post-infiltration. Scale bar=50 μm.

To further investigate the spatiotemporal expression pattern of *CsAGL6*, *in situ* hybridization was performed. Strong expression signals were observed in the four whorls of floral organ primordia during the early stages of flower bud development, but no significantly intense signal was detected in the shoot apical meristem (Fig. 3-A). At stage 1 (floral meristem, Fig. 3-B), expression was detected throughout the floral meristem. At stage 2 (sepal primordia initiation, Fig. 3-C), signals were localized to the developing sepal primordia. At stage 3 (sepal and petal primordia differentiation, Fig. 3-D and E), *CsAGL6* transcripts were found in both sepal and petal primordia. At stage 4 (development of sepal, petal, and stamen primordia, Fig. 3-F), strong signals were observed in all three primordia. At stage 5 (early carpel primordia formation, Fig. 3-G), transcripts were present in sepal, petal, stamen, and initiating carpel primordia. At stage 6 (Fig. 3-H), *CsAGL6* expression was detected in the primordia of petals, stamens, and dormant carpels. At stage 7 (Fig. 3-I), expression persisted in petal and stamen primordia, while at stage 8 (Fig. 3-J), signals were restricted to limited area of the stamen primordia in male buds. In female buds, *CsAGL6* was expressed in the four whorls of floral organ primordia, including the arrested stamen primordia, at stages 6 and 7 (Fig. 3-K). Additionally, expression was observed in the ovaries at stage 8 (Fig. 3-L). No hybridization signal was detected when the *CsAGL6* sense probe was used (Fig. 3-M and N). These findings

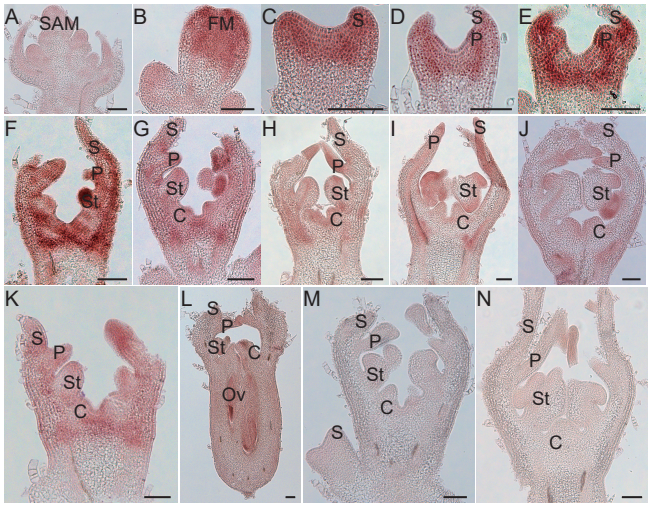


Fig. 3 Detection of *CsAGL6* expression in cucumber flower buds by *in situ* hybridization. A, shoot apex. B, stage 1 of flower bud. C, stage 2 of flower bud. D, stages 2–3 of flower bud. E, stage 3 of flower bud. F, stage 4 of flower bud. G, stage 5 of flower bud. H, stage 6 of male flower bud. I, stages 7–8 of male flower bud. J, stage 8 of male flower bud. K, stages 6–7 of female flower bud. L, stages 7–8 of female flower bud. M, negative control, stage 2 of flower bud and stage 6 of male flower bud. N, negative control, stages 8–9 of male flower bud. SAM, shoot apical meristem; FM, floral meristem; S, sepal; P, petal; St, stamen; C, carpel; Ov, ovary. Scale bar=100 μm.

suggest that *CsAGL6* may play a significant role in the development of the four whorls of floral organs during the early stages of flower bud development in cucumber.

3.3. Knocking out *CsAGL6* leads to greener petals and larger sepals

To explore the biological function of *CsAGL6*, we utilized the CRISPR/Cas9 system in combination with *Agrobacterium*-mediated genetic transformation to perform targeted genome editing and generated two homozygous mutant lines. The CR1 line exhibited a 1 bp deletion in exon 1, while the CR2 line displayed a compound deletion comprising 24 bp in exon 1 and 7 bp in intron 2, resulting in a total deletion of 31 bp (Fig. 4-A; Appendix D). These deletions induced frameshift mutations in the coding sequence (CDS) of the *CsAGL6* gene, leading to premature translational termination. Consequently, the CsAGL6 function was disrupted, with the mutations localized within the MADS-box domain (Fig. 4-A).

Through four seasons of continuous phenotypic observation, it was found that the petals of the two mutant lines exhibited a noticeably slower transition to yellow compared to the wild type (WT), with their color remaining greener at various stages of flower development (Fig. 4-B). Specifically, petals are green at the early flower bud stage but gradually transition to yellow as development progresses, resulting in fully bright yellow petals 1 d before and on the day of flowering in WT flowers (Fig. 4-B and C). In contrast, mutant petals remained entirely and distinctly green 1 d before flowering (Fig. 4-B), and on the flowering day, mutant petals turned yellow with only residual green pigmentation at the distal tips (Fig. 4-C). Since the stage of 1 d before flowering is the most reliable phase for distinguishing developmental differences, we measured chlorophyll content in petals at this time point to avoid potential misinterpretations

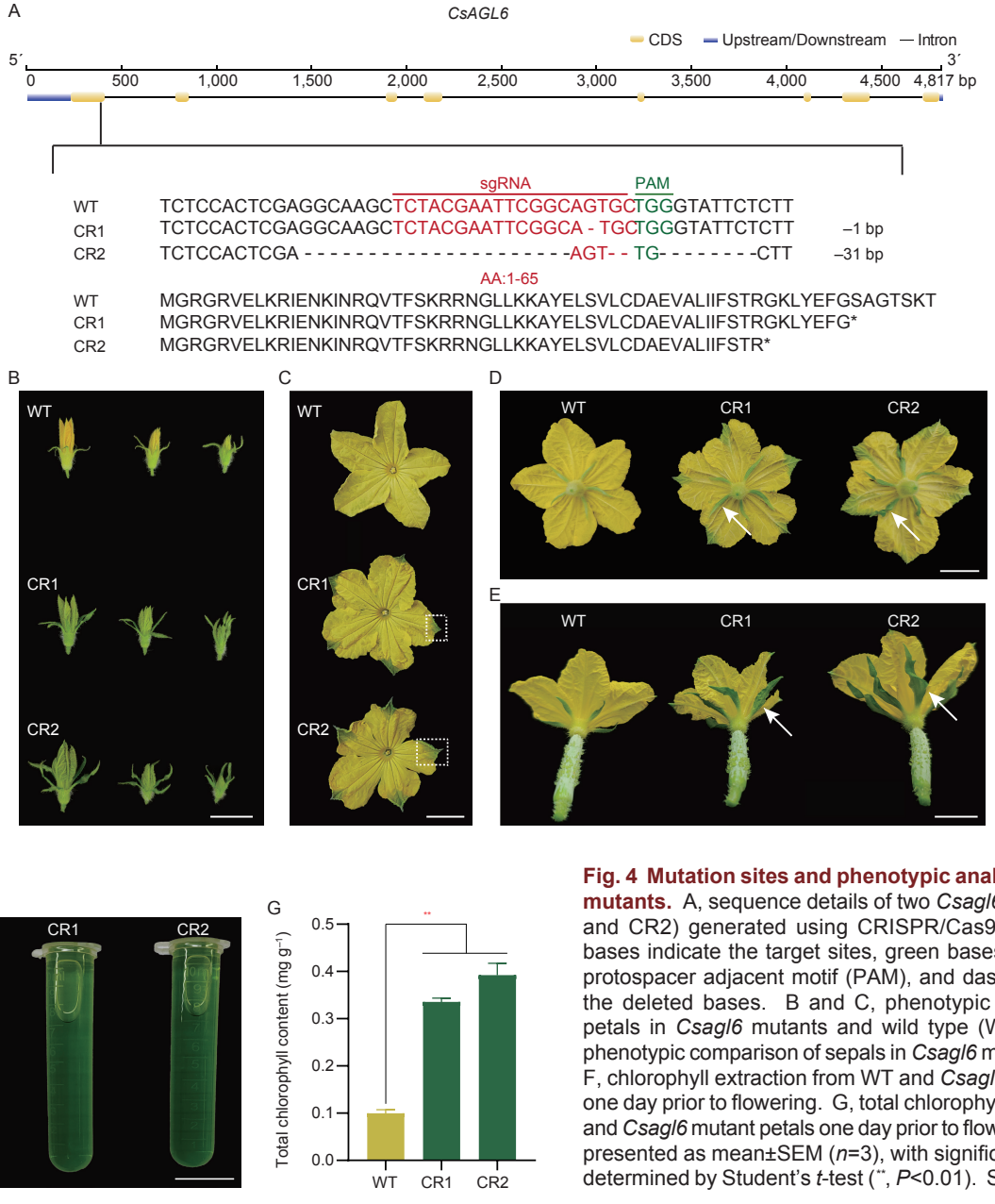


Fig. 4 Mutation sites and phenotypic analysis of *Csagl6* mutants. A, sequence details of two *Csagl6* mutants (CR1 and CR2) generated using CRISPR/Cas9 system. Red bases indicate the target sites, green bases represent the protospacer adjacent motif (PAM), and dashed lines mark the deleted bases. B and C, phenotypic comparison of petals in *Csagl6* mutants and wild type (WT). D and E, phenotypic comparison of sepals in *Csagl6* mutants and WT. F, chlorophyll extraction from WT and *Csagl6* mutant petals one day prior to flowering. G, total chlorophyll content in WT and *Csagl6* mutant petals one day prior to flowering. Data are presented as mean±SEM (n=3), with significant differences determined by Student's t-test (**, P<0.01). Scale bar=2 cm.

due to developmental asynchrony. Correspondingly, the total chlorophyll content in the petals of the mutant lines 1 d before flowering was significantly higher than that of the WT (Fig. 4-F and G). Moreover, the five petals of WT plants were regular in shape and uniform in size, whereas those of the mutant lines displayed abnormal morphology, with variability in shape and size (Fig. 4-C). Additionally, the sepals of the mutant male flowers (Fig. 4-D) and female flowers (Fig. 4-E) were slightly enlarged and exhibited a tendency towards leaf-like characteristics, but the enlarged sepal phenotype in mutants was only partially penetrant and restricted to early developmental stages, primarily at basal nodes. In general, the abnormalities in petals and sepals were more pronounced in the CR2 mutant line compared to the CR1 line. However, no significant differences were observed in the development of stamens and carpels between the WT and mutant plants.

3.4. *CsAGL6* regulates the expression of several A and E class, chlorophyll synthesis and chloroplast-mediated stress response related genes

To examine the role of *CsAGL6* in the development of cucumber sepals and petals, transcriptome sequencing was performed on the shoot apex of WT and *Csagl6* mutant plants. Pearson correlation coefficient analysis demonstrated that the correlation coefficients across all samples were at least 0.91, indicating a high degree of similarity in gene expression patterns and validating the high quality of the RNA-seq dataset (Appendix E). Differentially expressed genes (DEGs) were identified using a threshold of at least a two-fold difference in FPKM. In the CR1 lineage, 349 DEGs were identified, including 243 downregulated and 106 upregulated genes in the mutant (Appendices F and G). In the CR2 lineage, 696 DEGs were detected, comprising 475 downregulated and 221 upregulated genes in the mutant (Fig. 5-A; Appendix G).

Functional enrichment analysis of DEGs was conducted using the Kyoto Encyclopedia of Genes and Genomes (KEGG) and Gene Ontology (GO) databases. The KEGG enrichment analysis revealed significant enrichment in pathways related to chaperone-mediated folding catalysis and transcription factors (Fig. 5-D). Similarly, the GO enrichment analysis indicated significant enrichment in terms associated with protein folding, transcriptional regulation, and stress response (Fig. 5-E).

In the transcription factor pathway, several genes related to floral organ development, flowering time, and circadian rhythm regulation were found to be significantly enriched, with their transcript levels reduced in the mutants (Fig. 5-B). RT-qPCR analysis revealed that the expression of the A-class gene *AP1* and its homolog, *CAULIFLOWER* (*CAL*), which are involved in sepal and petal development (Theißen *et al.* 2016), was downregulated in both the CR1 and CR2 mutant lines. Notably, *CAL* exhibited a substantial decrease in expression, with a reduction of 40-fold in CR1 and 63-fold in CR2 (Fig. 5-F). Furthermore, the expression of the E-class gene *SEPALLATA4* (*SEP4*), which primarily regulates sepal development (Ditta *et al.* 2004), was also significantly downregulated in both mutant lines, showing a 1.4-fold decrease in CR1 and a 2-fold decrease in CR2 (Fig. 5-F). These findings suggest that *CsAGL6* may play a crucial role in the development of cucumber sepals and petals by modulating the expression of *CAL* and the E-class gene *SEP4*.

In the protein folding and stress response categories, several genes associated with chlorophyll synthesis and chloroplast-mediated stress responses were significantly enriched, and their transcripts were markedly upregulated in the mutant lines (Fig. 5-C). RT-qPCR analysis confirmed that the expression of *ELIP1* (*Early Light-Induced Protein 1*), a key gene involved in chlorophyll synthesis (Montané and Kloppstech 2000), was increased by 9.6-fold in the CR1 line and 16-fold in the CR2 line (Fig. 5-F). This suggests a higher accumulation of chlorophyll in the petals of the mutants, which could explain the persistent greening of the petals observed at all stages of flower development. Furthermore, the expression levels of *CPN60α1* (*chaperonin-60α1*), *CPN60β2* (*chaperonin-60β2*), *cpHsc70-2* (*chloroplast heat shock protein 70-2*), *CPN20* (*chaperonin 20*), as well as *EGY3* (*Ethylene-dependent Gravitropism-deficient and Yellow-green 3*), all essential for normal chloroplast development, were all significantly upregulated in both mutant lines (Fig. 5-F). These results suggest that the chloroplasts in the *Csagl6* mutants may be more robust, contributing to enhanced stress resistance in these plants.

4. Discussion

Flowers are essential reproductive organs in flowering plants. The fruits and seeds produced during flower development are vital food sources for humans. Additionally, the brightly colored floral organs have considerable ornamental value, and flowers of certain species are also known for their significant medicinal properties. Consequently, understanding flower development in angiosperms holds both theoretical and practical importance.

AGL6, an ancient MADS-box transcription factor, exhibits a conserved protein sequence across angiosperms, whereas its functions vary among species and may play pleiotropic roles within the same species. Regarding floral development, in *Arabidopsis*, *AGL6* loss-of-function mutants exhibited no visible phenotypic changes, but *Pro35S:AGL6* transgenic plants flowered very early in both long and short days with indicated increased expression of *FLOWERING LOCUS T* (*FT*) and *AP1* by RT-qPCR (Koo *et al.* 2010). New research findings indicated that the AGL6–ELF3 (EARLY FLOWERING 3)–FT circuit controls flowering time in *Arabidopsis*, in which, the AGL6 transcriptional repressor promotes floral transition by directly suppressing *ELF3*, which in turn directly represses *FT* expression, suggesting that AGL6 may activate *FT* expression in addition to the known FLC- and CONSTANS (CO)-dependent pathways during floral transition (Lee *et al.* 2024).

In petunia (*Petunia hybrida*), the *phagl6* single mutants exhibited no obvious phenotypic alterations, and the *fbp2* (an E-class gene) single mutants showed conversion of petals to green sepaloid tissue only at the edges of the petals. In contrast, *phagl6 fbp2* double mutants had completely

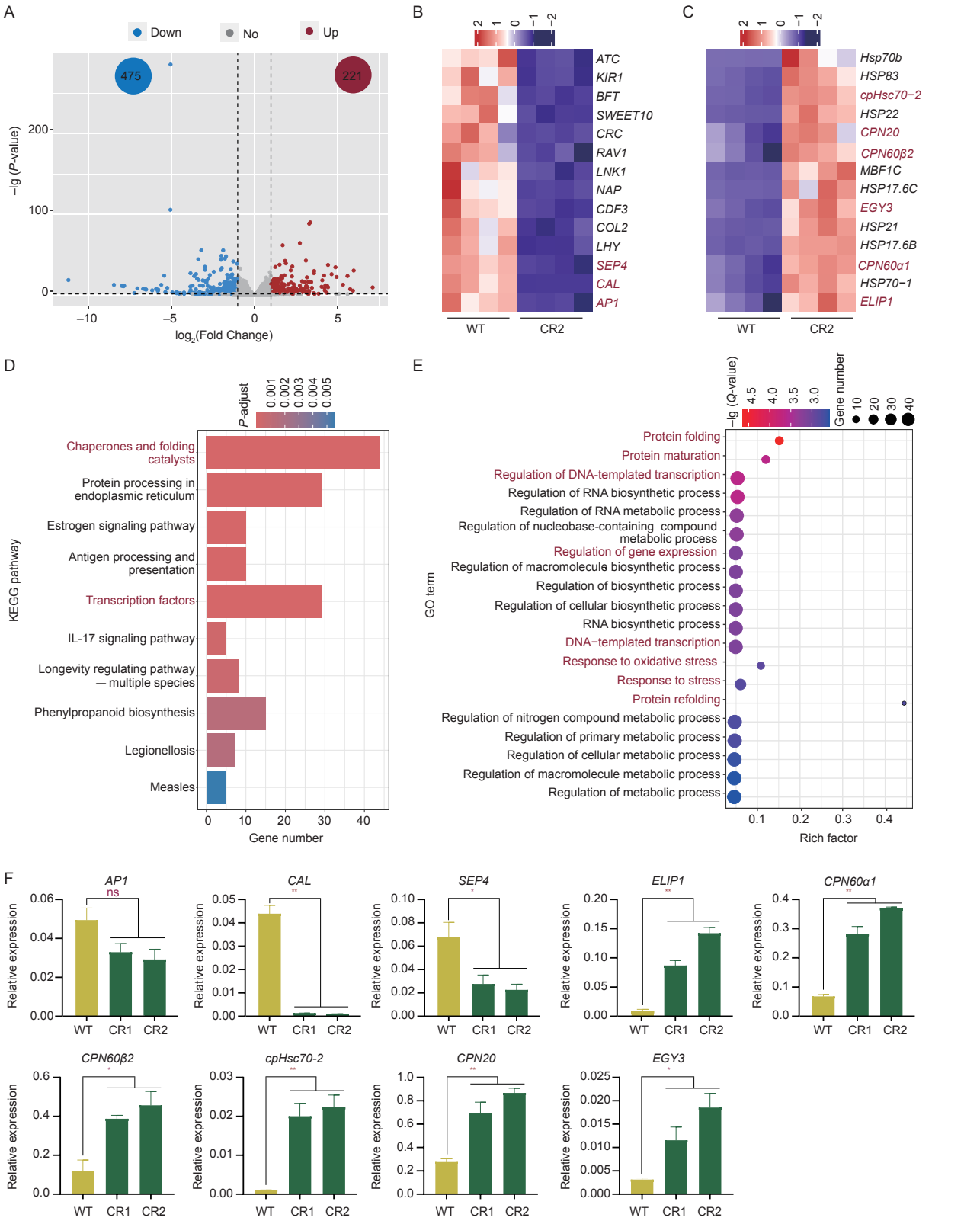


Fig. 5 RNA-seq data analysis and validation. A, volcano plot visualizing RNA-seq data of CR2 mutant line. Each point represents a gene. Blue and red points correspond to down-regulated and up-regulated genes, respectively, while gray points represent genes with no significant changes in expression. B and C, heatmaps showing the expression profiles of differentially expressed genes (DEGs) involved in flower development (B) and chloroplast-mediated stress response (C) in WT and CR2 mutant line. The color scale indicates relative gene expression levels across different samples, with purple to red representing increasing expression levels. D, KEGG pathway enrichment analysis of DEGs between WT and CR2 mutant line. E, GO term enrichment analysis of DEGs between WT and CR2 mutant line. F, RT-qPCR validation of down-regulated genes associated with sepal and petal development and up-regulated genes involved in chlorophyll synthesis and chloroplast development in *Csagl6* mutants. Data are presented as mean±SEM (n=3), with significant differences determined by Student's t-test (ns, non-significant; *, P<0.05; **, P<0.01).

green petals, and a corolla that was significantly reduced in size (Rijpkema *et al.* 2009). Further analysis revealed that both PhAGL6 and FBP2 interact with SUPPRESSOR OF OVEREXPRESSION OF CONSTANS 1 (SOC1)-clade proteins, C- and D-function proteins, as well as some other SEP-clade proteins (Rijpkema *et al.* 2009). In tomato, silencing *SlAGL6* resulted in abnormal fused sepals and pale-green petals with smaller size (Yu *et al.* 2017). Molecular analysis revealed that *MC* (an A-class gene regulating sepal identity), *GOBLET* (a NAC-domain gene involved in boundary establishment) and three B-class genes (*TM6*, *TAP3*, and *SlGLO1*) were down-regulated in transgenic petals. And two chlorophyll biosynthesis genes, *Golden2-like1* (*SlGLK1*) and *Golden2-like2* (*SlGLK2*), two photosystem-related genes, *ribulose bisphosphate carboxylase small chain 3B* (*SlrbcS3B*) and *chlorophyll a/b-binding protein 7* (*SlCab-7*) were up-regulated in transgenic petals (Yu *et al.* 2017).

In rice, *OsMADS17* played minor and redundant roles, whereas allelic mutants of *OsMADS6* exhibited severe defects in flower development and the mutation of *OsMADS1* (a SEP-like gene) enhanced the defect of *Osmads6* (Ohmori *et al.* 2009; Li *et al.* 2010). Later studies indicated that OsMADS6 directly promotes *FACTOR OF DNA METHYLATION LIKE 1* (*OsFDML1*) expression through binding to regions containing putative CArG motifs within the *OsFDML1* promoter during rice spikelet development (Tao *et al.* 2018). In hexaploidy wheat, stamens of the *TaAGL6* RNAi plants (*TaAGL6-A*, *TaAGL6-B* and *TaAGL6-D* were knocked down simultaneously) showed abnormality in number and morphology with the *TaAP3* downregulated (Su *et al.* 2019). Yeast one hybrid and transient expression assays showed that TaAGL6 positively regulates the expression of *TaAP3 in vivo* and the results of yeast two-hybrid (Y2H) and bimolecular fluorescence complementation (BiFC) assays indicated that TaAGL6 interacts with TaAP3, TaAG (AGAMOUS) and TaMADS13 (Su *et al.* 2019). Further studies showed that tetraploid wheat *ttagl6-A* and *ttagl6-B* homozygous single mutants exhibited no significant vegetative or spike anomaly except for reduced grain number per spike. In contrast, *ttagl6-A ttagl6-B* double mutants were completely sterile and all four floral whorls exhibit serious abnormalities (Kong *et al.* 2022). Multiple A-, B-, C-, and D-class genes showed altered expression patterns and yeast two-hybrid analyses detected interactions of TaAGL6 with all classes of MADS-box proteins in the ABCDE model (Kong *et al.* 2022).

In our study, the expression pattern analysis of *CsAGL6* revealed that it is predominantly expressed in flowers. In *Csagl6* mutants, the petal color is consistently greener than that of the wild type across all stages of flower development, and both petal shape and size are abnormal. Additionally, during early developmental stages, some flowers exhibit occasional sepal enlargement and leaf-like characteristics at basal nodal positions. These phenotypic abnormalities suggest that *CsAGL6* plays a role in regulating the development of cucumber sepals and petals. According to the ABCDE model of floral organ development, A- and E-class genes jointly regulate sepal development, while A-, B-, and E-class genes collectively control petal development. Transcriptome analysis revealed that in *Csagl6* mutants, the expression of A-class genes *AP1* and *CAL*, as well as the E-class gene *SEP4*, is significantly downregulated. This downregulation likely contributes to the observed abnormalities in the sepals and petals of the mutants, indicating that *CsAGL6* may regulate the development of these organs by modulating A- and E-class gene expression.

Chlorophyll serves as the central pigment in photosynthesis and is found not only in mesophyll cells but also in other tissues responsible for tissue coloration. For instance, recent studies have shown that overexpression of *CONSTANS-LIKE 1* (*SlCOL1*) leads to a significant increase in chlorophyll content in immature tomato fruits, resulting in darker fruit color (Cui *et al.* 2025), while suppression of *Green hypocotyl color 1* (*CmGhc1*) reduces chlorophyll levels in melon hypocotyls, causing them to turn white (Yang *et al.* 2025). In this study, petals of the *Csagl6* mutant exhibited higher chlorophyll content compared to the wild type, leading to a greener petal appearance. The transcriptome analysis results indicate a significant upregulation of *ELIP1* expression in the *Csagl6* mutant. ELIP1, a chlorophyll *a*/*b*-binding protein, is known to play a key role in regulating chlorophyll biosynthesis (Montané and Kloppstech 2000). In *Arabidopsis*, the chlorophyll contents of *elip1* mutants and *elip1 elip2* double mutants were all lower than that of wild type, showing a slightly pale green phenotype during greening of etiolated seedlings in continuous light (Casazza *et al.* 2005; Rossini *et al.* 2006). Recent studies have shown that white light promotes chlorophyll biosynthesis by enhancing *ELIP1* expression, thereby extending the shelf life of Chinese cabbage (Wang *et al.* 2022). The marked upregulation of *ELIP1* in the *Csagl6* mutants suggests increased chlorophyll accumulation in their petals, which is supported by measurements showing that chlorophyll content in the mutant petals is significantly higher than in WT petals. As a result, the petal color of the mutants appears greener.

Moreover, the expression levels of *CPN60α1*, *CPN60β2*, *cpHsc70-2*, *CPN20* and *EGY3* are significantly elevated in the *Csagl6* mutant. *CPN60α1* and *CPN60β2* encodes a subunit of chloroplast chaperonin CPN60 respectively, which is involved in folding of newly synthesized, translocated, or stress-denatured proteins (Viitanen *et al.* 1995; Dickson *et al.* 2000). In *Arabidopsis*, *cpn60α1* mutants exhibit abnormalities such as defective embryos, short etiolated seedlings, decreased chlorophyll content and chloroplasts in leaves; and the *cpn60β1 cpn60β2* double mutant shows yellowing of young leaves, dwarfism, and stunted growth (Apuya *et al.* 2001; Suzuki *et al.* 2009). These results suggest that both *CPN60α1* and *CPN60β2* are required for the normal division and development of chloroplasts. *cpHsc70-2* encodes a chloroplast-localized heat shock protein that is essential for the normal development and function of chloroplasts, with a white and stunted phenotype in *Arabidopsis* in which *cpHsc70-1* and *cpHsc70-2* are silenced simultaneously (Latijnhouwers *et al.* 2010). *CPN20* encodes a chloroplast co-chaperonin, mediating iron superoxide dismutase activity in *Arabidopsis* chloroplasts (Kuo *et al.* 2013). In addition, down-expression of *CPN20* increases, but overexpression of *CPN20* reduces abscisic acid sensitivity (Zhang *et al.*

2013). *EGY3* encodes a protein localized to the chloroplast thylakoid membrane (Adamiec *et al.* 2020), where it plays a key role in mediating chloroplast reactive oxygen species (ROS) homeostasis and the response to abiotic stresses, including high light, elevated temperature, and salt stress by promoting the Cu/Zn-superoxide dismutase 2 stability and H_2O_2-mediated chloroplastic retrograde signaling (Zhuang *et al.* 2021; Adamiec *et al.* 2022). The marked increase in the transcript levels of these chloroplast-associated stress response genes suggests that the *Csagl6* mutants may possess enhanced photosynthetic and stress response capabilities. However, further experimental validation is required to confirm these findings.

To further strengthen the conjectures regarding the molecular mechanism of *CsAGL6* regulating sepal and petal development in cucumber, we performed promoter analyses in PlantPAN 4.0 website (https://plantpan.itps.ncku.edu.tw/plantpan4/index.html). Notably, considerable putative AGL6 transcription factor binding sites are identified in the promoter regions of these chlorophyll biosynthesis-/chloroplast development-related genes and floral organ identity genes *CAL* and *SEP4*, all of which show significant expression changes in the *Csagl6* mutants (Appendix H). Furthermore, the promoters of *CAL* and *HSP21* contain experimentally validated AGL6 binding regions supported by DAP-seq in *Arabidopsis* (Appendix H). Based on these findings, we propose that *CsAGL6* may regulate petal coloration by binding to the promoters of chlorophyll-/chloroplast-related genes to suppress their expression, while it likely activates *CAL* and *SEP4* to influence sepal and petal development. Given that MADS proteins typically function as homodimers or heteromeric complexes, and considering the research results of *AGL6* in floral development across species, we hypothesize that *CsAGL6* exerts its regulatory effects by forming multimeric complexes with other MADS-box proteins.

5. Conclusion

Our study demonstrates that *CsAGL6* is highly expressed in cucumber flowers and likely plays a role in the development of sepals and petals by regulating the expression of A-class and E-class related genes. Additionally, it appears to influence chlorophyll synthesis and chloroplast development through the regulation of associated genes. These findings offer valuable insights into the molecular mechanisms underlying cucumber flower development and contribute to the understanding of functional differentiation within the *AGL6* subfamily genes in the Cucurbitaceae family.

Acknowledgements

This work was supported by funding from the National Natural Science Foundation of China (32222075 and 32472768) and the Science and Technology Innovation Program of the Chinese Academy of Agricultural Sciences (CAAS-ASTIP-2024-IVF).

Declaration of competing interest

The authors declare that they have no conflict of interest.

Declaration of generative AI and AI-assisted technologies in the writing process

During the preparation of this manuscript, the authors used ChatGPT 4.0 to assist in improving the clarity and readability of the language. All content generated was carefully reviewed and revised by the authors as necessary, and the authors take full responsibility for the final content of the article.

Appendices associated with this paper are available at https://doi.org/10.1016/j.jia.2025.11.012

References

Adamiec M, Dobrogojski J, Wojtyla Ł, Luciński R. 2022. Stress-related expression of the chloroplast EGY3 pseudoprotease and its possible impact on chloroplasts' proteome composition. *Frontiers in Plant Science*, **13**, 965143.

Adamiec M, Misztal L, Kasprowicz-Maluśki A, Luciński R. 2020. EGY3: Homologue of S2P protease located in chloroplasts. *Plant Biology*, **22**, 735–743.

Angenent G C, Colombo L. 1996. Molecular control of ovule development. *Trends in Plant Science*, **1**, 228–232.

Apuya N R, Yadegari R, Fischer R L, Harada J J, Zimmerman J L, Goldberg R B. 2001. The *Arabidopsis* embryo mutant *schlepperless* has a defect in the *chaperonin-60α* gene. *Plant Physiology*, **126**, 717–730.

Becker A, Theissen G. 2003. The major clades of MADS-box genes and their role in the development and evolution of flowering plants. *Molecular Phylogenetics and Evolution*, **29**, 464–489.

Bowman J L, Smyth D R, Meyerowitz E M. 2012. The ABC model of flower development: Then and now. *Development*, **139**, 4095–4098.

Casazza A P, Rossini S, Rosso M G, Soave C. 2005. Mutational and expression analysis of *ELIP1* and *ELIP2* in *Arabidopsis thaliana*. *Plant Molecular Biology*, **58**, 41–51.

Causier B, Schwarz-Sommer Z, Davies B. 2010. Floral organ identity: 20 years of ABCs. *Seminars in Cell & Development Biology*, **21**, 73–79.

Coen E S, Meyerowitz E M. 1991. The war of the whorls: Genetic interactions controlling flower development. *Nature*, **353**, 31–37.

Cui L, Zheng F Y, Zhang C H, Gao S N, Ye J, Zhang Y Y, Wang T T, Hong Z L, Ye Z B, Zhang J H. 2025. The CONSTANS-LIKE SlCOL1 in tomato regulates the fruit chlorophyll content by stabilizing the GOLDEN2-LIKE protein. *Journal of Integrative Agriculture*, **24**, 536–545.

Dickson R, Weiss C, Howard R J, Alldrick S P, Ellis R J, Lorimer G, Azem A, Viitanen P V. 2000. Reconstitution of higher plant chloroplast chaperonin 60 tetradecamers active in protein folding. *Journal of Biological Chemistry*, **275**, 11829–11835.

Ditta G, Pinyopich A, Robles P, Pelaz S, Yanofsky M F. 2004. The *SEP4* gene of *Arabidopsis thaliana* functions in floral organ and meristem identity. *Current Biology*, **14**, 1935–1940.

Dreni L, Zhang D. 2016. Flower development: The evolutionary history and functions of the *AGL6* subfamily MADS-box genes. *Journal of Experiment Botany*, **67**, 1625–1638.

Duan Y, Xing Z, Diao Z, Xu W, Li S, Du X, Wu G, Wang C, Lan T, Meng Z, Liu H, Wang F, Wu W, Xue Y. 2012. Characterization of *Osmads6-5*, a null allele, reveals that *OsMADS6* is a critical regulator for early flower development in rice (*Oryza sativa* L.). *Plant Molecular Biology*, **80**, 429–442.

Elliot M M, David R S, John L B. 1989. Abnormal flowers and pattern formation in floral development. *Development*, **106**, 209–217.

Favaro R, Pinyopich A, Battaglia R, Kooiker M, Borghi L, Ditta G, Yanofsky M F, Kater M M, Colombo L. 2003. MADS-box protein complexes control carpel and ovule development in Arabidopsis. *The Plant Cell*, **15**, 2603–2611.

Hileman L C, Sundstrom J F, Litt A, Chen M, Shumba T, Irish V F. 2006. Molecular and phylogenetic analyses of the MADS-box gene family in tomato. *Molecular Biology and Evolution*, **23**, 2245–2258.

Hsu H F, Chen W H, Shen Y H, Hsu W H, Mao W T, Yang C H. 2021. Multifunctional evolution of B and *AGL6* MADS box genes in orchids. *Nature Communications*, **12**, 902.

Hsu W H, Yeh T J, Huang K Y, Li J Y, Chen H Y, Yang C H. 2014. *AGAMOUS-LIKE13*, a putative ancestor for the E functional genes, specifies male and female gametophyte morphogenesis.

The Plant Journal, **77**, 1–15.
Huang X, Effgen S, Meyer R C, Theres K, Koornneef M. 2012. Epistatic natural allelic variation reveals a function of *AGAMOUS-LIKE6* in axillary bud formation in *Arabidopsis*. *The Plant Cell*, **24**, 2364–2379.
Irish V F. 2010. The flowering of *Arabidopsis* flower development. *The Plant Journal*, **61**, 1014–1028.
Klap C, Yeshayahou E, Bolger A M, Arazi T, Gupta S K, Shabtai S, Usadel B, Salts Y, Barg R. 2017. Tomato facultative parthenocarpy results from *SlAGAMOUS-LIKE 6* loss of function. *Plant Biotechnology Journal*, **15**, 634–647.
Kong X, Wang F, Geng S, Guan J, Tao S, Jia M, Sun G, Wang Z, Wang K, Ye X, Ma J, Liu D, Wei Y, Zheng Y, Fu X, Mao L, Lan X, Li A. 2022. The wheat *AGL6-like* MADS-box gene is a master regulator for floral organ identity and a target for spikelet meristem development manipulation. *Plant Biotechnology Journal*, **20**, 75–88.
Koo S C, Bracko O, Park M S, Schwab R, Chun H J, Park K M, Seo J S, Grbic V, Balasubramanian S, Schmid M, Godard F, Yun D J, Lee S Y, Cho M J, Weigel D, Kim M C. 2010. Control of lateral organ development and flowering time by the *Arabidopsis thaliana* MADS-box Gene *AGAMOUS-LIKE6*. *The Plant Journal*, **62**, 807–816.
Kuo W Y, Huang C H, Liu A C, Cheng C P, Li S H, Chang W C, Weiss C, Azem A, Jinn T L. 2013. CHAPERONIN 20 mediates iron superoxide dismutase (FeSOD) activity independent of its co-chaperonin role in *Arabidopsis* chloroplasts. *New Phytologist*, **197**, 99–110.
Latijnhouwers M, Xu X M, Møller S G. 2010. *Arabidopsis* stromal 70-kDa heat shock proteins are essential for chloroplast development. *Planta*, **232**, 567–578.
Lee K, Yoon H, Seo P J. 2024. The AGL6-ELF3-FT circuit controls flowering time in *Arabidopsis*. *Plant Signaling & Behavior*, **19**, 2358684.
Li B J, Zheng B Q, Wang J Y, Tsai W C, Lu H C, Zou L H, Wan X, Zhang D Y, Qiao H J, Liu Z J, Wang Y. 2020. New insight into the molecular mechanism of colour differentiation among floral segments in orchids. *Communications Biology*, **3**, 89.
Li H, Liang W, Jia R, Yin C, Zong J, Kong H, Zhang D. 2010. The *AGL6-like* gene *OsMADS6* regulates floral organ and meristem identities in rice. *Cell Research*, **20**, 299–313.
Mizukami Y, Ma H. 1992. Ectopic expression of the floral homeotic gene *AGAMOUS* in transgenic Arabidopsis plants alters floral organ identity. *Cell*, **71**, 119–131.
Montané M H, Kloppstech K. 2000. The family of light-harvesting-related proteins (LHCs, ELIPs, HLIPs): Was the harvesting of light their primary function? *Gene*, **258**, 1–8.
Ohmori S, Kimizu M, Sugita M, Miyao A, Hirochika H, Uchida E, Nagato Y, Yoshida H. 2009. *MOSAIC FLORAL ORGANS1*, an *AGL6-like* MADS box gene, regulates floral organ identity and meristem fate in rice. *The Plant Cell*, **21**, 3008–3025.
Pelaz S, Ditta G S, Baumann E, Wisman E, Yanofsky M F. 2000. B and C floral organ identity functions require *SEPALLATA* MADS-box genes. *Nature*, **405**, 200–203.
Pelaz S, Tapia-López R, Alvarez-Buylla E R, Yanofsky M F. 2001. Conversion of leaves into petals in Arabidopsis. *Current Biology*, **11**, 182–184.
Peng S M, Luo T, Zhou J Y, Niu B, Lei N F, Tang L, Chen F. 2008. Cloning and quantification of expression levels of two MADS-box genes from *Momordica charantia*. *Biologia Plantarum*, **52**, 222–230.
Pinyopich A, Ditta G S, Savidge B, Liljegren S J, Baumann E, Wisman E, Yanofsky M F. 2003. Assessing the redundancy of MADS-box genes during carpel and ovule development. *Nature*, **424**, 85–88.
Purugganan M D. 1997. The MADS-box floral homeotic gene lineages predate the origin of seed plants: Phylogenetic and molecular clock estimates. *Journal of Molecular Evolution*, **45**, 392–396.
Rijpkema A S, Zethof J, Gerats T, Vandenbussche M. 2009. The petunia *AGL6* gene has a *SEPALLATA*-like function in floral patterning. *The Plant Journal*, **60**, 1–9.
Rossini S, Casazza A P, Engelmann E C, Havaux M, Jennings R C, Soave C. 2006. Suppression of both *ELIP1* and *ELIP2* in *Arabidopsis* does not affect tolerance to photoinhibition and photooxidative stress. *Plant Physiology*, **141**, 1264–1273.
Schmittgen T D, Livak K J. 2008. Analyzing real-time PCR data by the comparative C_T method. *Nature Protocols*, **3**, 1101–1108.
Su Y, Liu J, Liang W, Dou Y, Fu R, Li W, Feng C, Gao C, Zhang D, Kang Z, Li H. 2019. Wheat AGAMOUS LIKE 6 transcription factors function in stamen development by regulating the expression of *TaAPETALA3*. *Development*, **146**, dev177527.
Suzuki K, Nakanishi H, Bower J, Yoder D W, Osteryoung K W, Miyagishima S Y. 2009. Plastid chaperonin proteins Cpn60α and Cpn60β are required for plastid division in *Arabidopsis thaliana*. *BMC Plant Biology*, **9**, 38.
Tao J, Liang W, An G, Zhang D. 2018. *OsMADS6* controls flower development by activating rice *FACTOR OF DNA METHYLATION LIKE1*. *Plant Physiology*, **177**, 713–727.
Theißen G. 2001. Development of floral organ identity: Stories from the MADS house. *Current Opinion in Plant Biology*, **4**, 75–85.
Theißen G, Melzer R, Rümpler F. 2016. MADS-domain transcription factors and the floral quartet model of flower development: Linking plant development and evolution. *Development*, **143**, 3259–3271.
Viaene T, Vekemans D, Becker A, Melzer S, Geuten K. 2010. Expression divergence of the AGL6 MADS domain transcription factor lineage after a core eudicot duplication suggests functional diversification. *BMC Plant Biology*, **10**, 148.
Viitanen P V, Schmidt M, Buchner J, Suzuki T, Vierling E, Dickson R, Lorimer G H, Gatenby A, Soll J. 1995. Functional characterization of the higher plant chloroplast chaperonins. *Journal of Biological Chemistry*, **270**, 18158–18164.
Wang C, Sun J J, Yang X Y, Wan L, Zhang Z H, Zhang H M. 2023. An optimized protocol using Steedman's wax for high-sensitivity RNA *in situ* hybridization in shoot apical meristems and flower buds of cucumber. *Journal of Integrative Agriculture*, **22**, 464–470.
Wang T, Liu S, Tian S, Ma T, Wang W. 2022. Light regulates chlorophyll biosynthesis via ELIP1 during the storage of Chinese cabbage. *Scientific Reports*, **12**, 11098.
Xin T, Tian H, Ma Y, Wang S, Yang L, Li X, Zhang M, Chen C, Wang H, Li H, Xu J, Huang S, Yang X. 2022. Targeted creating new mutants with compact plant architecture using CRISPR/Cas9 genome editing by an optimized genetic transformation procedure in cucurbit plants. *Horticulture Research*, **9**, uhab086.
Xing H L, Dong L, Wang Z P, Zhang H Y, Han C Y, Liu B, Wang X C, Chen Q J. 2014. A CRISPR/Cas9 toolkit for multiplex genome editing in plants. *BMC Plant Biology*, **14**, 327.
Yang Y, Fan R, Zhang X J, Li M H, Zhang Y B, Yi H P, Ma M R, Yang Y, Liu B, Liu X W, Ren H Z. 2025. Mutation in *CmGhc1* confers the white hypocotyl phenotype in melon (*Cucumis melo* L.). *Journal of Integrative Agriculture*, **24**, 4242–4254.
Yoo S K, Hong S M, Lee J S, Ahn J H. 2011. A genetic screen for leaf movement mutants identifies a potential role for *AGAMOUS-LIKE 6* (*AGL6*) in circadian-clock control. *Molecules and Cells*, **31**, 281–287.
Yu X, Chen G, Guo X, Lu Y, Zhang J, Hu J, Tian S, Hu Z. 2017. Silencing *SlAGL6*, a tomato *AGAMOUS-LIKE6* lineage gene, generates fused sepal and green petal. *Plant Cell Reports*, **36**, 959–969.
Yu X, Duan X, Zhang R, Fu X, Ye L, Kong H, Xu G, Shan H. 2016. Prevalent exon-intron structural changes in the *APETALA1*/*FRUITFULL*, *SEPALLATA*, *AGAMOUS-LIKE6*, and *FLOWERING LOCUS C* MADS-Box gene subfamilies provide new insights into their evolution. *Frontiers in Plant Science*, **7**, 598.
Yu X, Xia S, Xu Q, Cui Y, Gong M, Zeng D, Zhang Q, Shen L, Jiao G, Gao Z, Hu J, Zhang G, Zhu L, Guo L, Ren D, Qian Q. 2020. *ABNORMAL FLOWER AND GRAIN 1* encodes OsMADS6 and determines palea identity and affects rice grain yield and quality. *Science China Life Sciences*, **63**, 228–238.
Zhang X F, Jiang T, Wu Z, Du S Y, Yu Y T, Jiang S C, Lu K, Feng X J, Wang X F, Zhang D P. 2013. Cochaperonin CPN20 negatively regulates abscisic acid signaling in *Arabidopsis*. *Plant Molecular Biology*, **83**, 205–218.
Zhuang Y, Wei M, Ling C, Liu Y, Amin AK, Li P, Li P, Hu X, Bao H, Huo H, Smalle J, Wang S. 2021. EGY3 mediates chloroplastic ROS homeostasis and promotes retrograde signaling in response to salt stress in *Arabidopsis*. *Cell Reports*, **36**, 109384.

Executive Editor-in-Chief Sanwen Huang
Managing Editor Lingyun Weng